SF2A 2021
A. Siebert, K. Baillié, E. Lagadec, N. Lagarde, J. Malzac, J.-B. Marquette, M. N'Diaye, J. Richard, O. Venot (eds)

CHARACTERISING THE INTERIOR STRUCTURES AND ATMOSPHERES OF MULTIPLANETARY SYSTEMS

L. Acuña[1], T. Lopez[1], M. Deleuil[1], O. Mousis[1], E. Marcq[2], T. Morel[3] and A. Santerne[1]

Abstract. The modelling of the internal structures of super-Earths and sub-Neptunes gives a valuable insight into their formation history and possible atmospheres. We present a planet model where the interior is coupled with the atmosphere within a Bayesian retrieval scheme. We take into account water in all its possible phases, including steam and supercritical phases, which is necessary for systems with a wide range of stellar irradiations. Our interior-atmosphere model calculates the compositional and atmospheric parameters, such as Fe and water content, surface pressures, scale heights and albedos. We analyse the multiplanetary systems K2-138 and TRAPPIST-1. From their individual composition, we derive a global increasing trend on the water content with increasing distance from the star in the inner region of the systems, while the planets in the outer region present a constant water mass fraction. This trend reveals the possible effects of migration, formation location and atmospheric mass loss during their formation history.

Keywords: Planets and satellites: interiors, Planets and satellites: composition, Planets and satellites: atmospheres, Planets and satellites: individual: K2-138, Stars: activity.

1 Introduction

Multiplanetary systems show a diversity in the composition of their planets, ranging from rocky super-Earths to volatile-rich sub-Neptunes. This variety in composition makes multiplanetary systems environments that are interesting for testing theories on planet formation and evolution. Two examples of multiplanetary systems of low-mass planets (M ¡ 20 $M_\oplus$) with different densities are TRAPPIST-1 (Gillon et al. 2016; Agol et al. 2021) and K2-138 (Christiansen et al. 2018; Lopez et al. 2019). In this work we present a homogeneous interior-atmosphere analysis of the planets in these two systems to unveil their compositional trends. We also discuss how interior structure and composition studies of low-mass planets can be impacted by stellar activity.

2 Interior-atmosphere analysis

2.1 Interior model

The interior structure model is initially presented in Brugger et al. (2016) and Brugger et al. (2017). It is a one-dimensional model that takes as input the total planetary mass, two compositional parameters and the surface pressure and temperature. The two compositional parameters are the core mass fraction (CMF) and water mass fraction (WMF), which are the mass of the core and the water layer, respectively, divided by the total mass of the planet. Along the one-dimensional grid, which represents the radius, we calculate the pressure $P(r)$, gravity $g(r)$, temperature $T(r)$ and density $\rho(r)$. We finally obtain as output the total planetary radius and the Fe/Si mole ratio.

The planet is stratified in three main layers: a Fe-rich core, a Si-dominated mantle and a water layer. Depending on the water phase, we use a different equation of state (EOS) that is valid under the pressure and temperature conditions of that phase. Brugger et al. (2016) and Brugger et al. (2017) implemented liquid and

[1] Aix Marseille Univ, CNRS, CNES, LAM, Marseille, France
[2] LATMOS/CNRS/Sorbonne Université/UVSQ, 11 boulevard d'Alembert, Guyancourt, F-78280, France
[3] Space sciences, Technologies and Astrophysics Research (STAR) Institute, Université de Liège, Quartier Agora, Allée du 6 Août 19c, Bât. B5C, B4000-Liège, Belgium

ice phases, which are valid for temperate planets. Nonetheless, many of the planets in multiplanetary systems are highly irradiated, having surface conditions that do not allow for the formation of liquid and ice phases. Therefore we update our interior structure model to include the supercritical phase (Mousis et al. 2020). We use an EOS that is valid for high-pressure, high-temperature conditions in supercritical phase from Mazevet et al. (2019).

In addition, we couple the interior with the atmosphere self-consistently. We use a one-dimensional, k-correlated model, described in Marcq (2012) and Marcq et al. (2017). The interface between the atmosphere and the interior, which is either the supercritical layer or the mantle, is situated at P = 300 bar. The atmospheric model calculates the thickness of the atmosphere, which contributes significantly to the total radius, with an EOS that is valid for water vapour conditions. Furthermore, the atmospheric model also obtains the outgoing longwave radiation (OLR) and Bond albedo, which enable us to estimate the temperature at the bottom of the atmosphere assuming radiative-convective equilibrium. The temperature at the bottom of the atmosphere is the input boundary condition for the interior. We developed an algorithm to couple self-consistently the interior and the atmosphere, described in Acuña et al. (2021). This implementation of the supercritical interior and atmosphere allows us to obtain smooth pressure-temperature profiles of the water layer (Fig. 1).

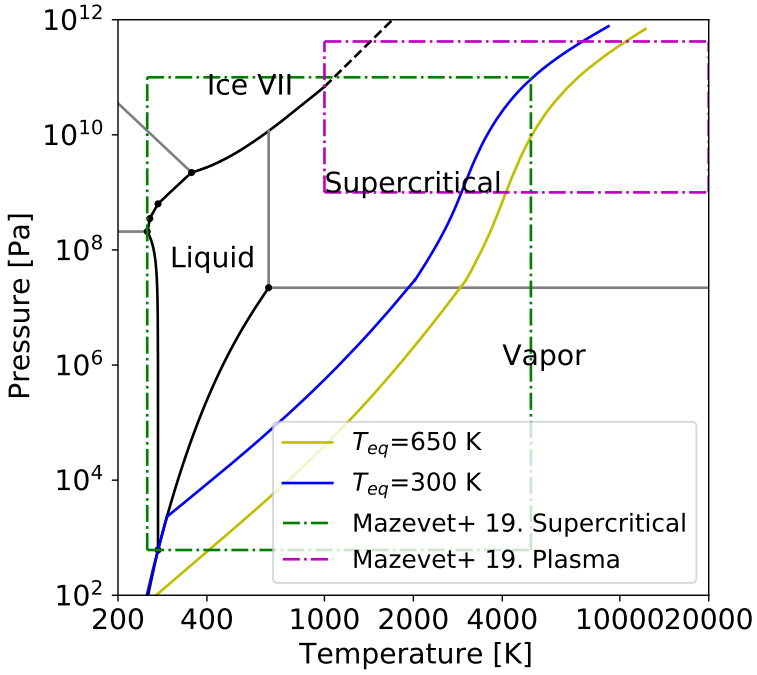

Fig. 1. Pressure-temperature profiles of the water layer for our interior-atmosphere model for highly irradiated planets. The two profiles correspond to two hypothetical planets with M = 15 $M_{\oplus}$ and 100% water composition for two different equilibrium temperatures. Green and magenta dashed-dotted boxes indicate the validity ranges of the supercritical EOS from Mazevet et al. (2019).

2.2 Observational parameters

We use a Bayesian MCMC scheme, described in Dorn et al. (2015) and Acuña et al. (2021), to obtain the non-observable parameters (CMF and WMF) and their uncertainties, while having as input the observables, which are the planetary mass and radius, and the Fe/Si mole ratio. The latter is estimated with the host stellar abundances, as defined in Sotin et al. (2007) and Brugger et al. (2017). For K2-138, we perform our own spectroscopic analysis to obtain refined planetary masses, stellar parameters and abundances (Acuña et al. in prep). In the case of TRAPPIST-1, we employ masses and radii reported in Agol et al. (2021) and the Fe/Si mole ratio estimated by Unterborn et al. (2018), Fe/Si = 0.76 ± 0.12. This estimate is obtained by selecting a sample of stars with similar metallicity to TRAPPIST-1 and available Fe and Si abundances.

3 Results

We observe that the WMF trend in K2-138 consists of an increasing gradient with increasing distance from the star (or incident flux) for the three inner planets, whereas the three outer planets have a constant WMF (a plateau). In addition, the outermost planet, K2-138 g, has a radius that is significantly larger than the radius we obtain with our interior-atmosphere modelling, assuming 100% water atmosphere. This indicates that the atmosphere of K2-138 g is composed of species that are more volatile than water, and therefore produce a more extended atmosphere than a water-dominated one. These species are H and He, which means that they have survived atmospheric loss due to XUV photoevaporation, while for the other planets in the K2-138 this is not the case. This WMF trend is also seen in TRAPPIST-1 (Fig. 2), where planets b to e have increasing WMF and planets f to g have a constant WMF of 15% approximately. TRAPPIST-1 d seems to be the exception to this trend. However, in Acuña et al. (2021) we discuss that this could be due to assuming that the water layer in TRAPPIST-1 d is in liquid phase. If CO_2 is mixed with water vapour in the atmosphere, this would not allow the presence of liquid water in TRAPPIST-1 d. Since the density of water vapour is lower than liquid water, a lower WMF is needed to account for the total density of the planet. This shifts downwards the position of TRAPPIST-1 d in Fig. 2, placing it between that of TRAPPIST-1 c and e (Acuña et al. 2021; Turbet et al. 2020)

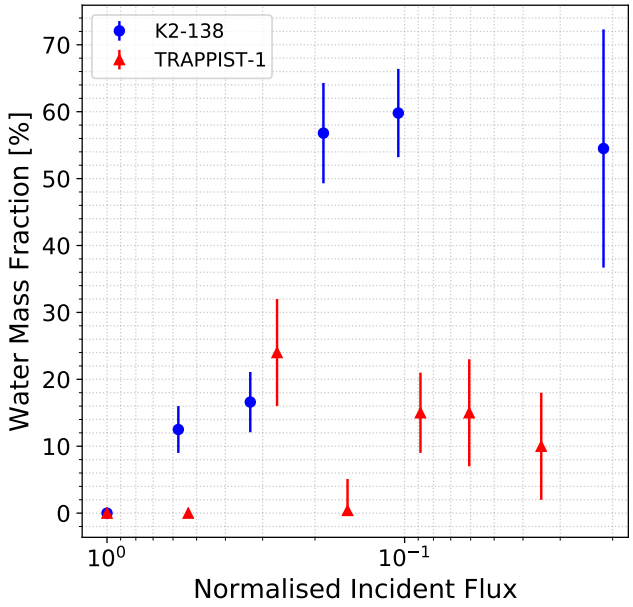

Fig. 2. WMF trend as a function of normalised incident flux for K2-138 and TRAPPIST-1. The incident flux is normalised with the flux of the innermost planet in each planetary system.

4 Discussion

The uncertainty in radius due to stellar activity for a Jupiter-size planet is 3% (Czesla et al. 2009), which translates into a larger uncertainty in the case of small planets. The uncertainty in radius necessary to distinguish a super-Earth from a sub-Neptune is 10% for planets with M ¿ 10 $M_\oplus$, 5% for masses between 5 and 10 $M_\oplus$, and less than 5% for planets less massive than 5 $M_\oplus$ (Wagner et al. 2011). Therefore, we need accurate stellar activity modelling to obtain radii within these uncertainties, especially for Earth-size planets. This requires observations of several stellar rotations and models for stellar granulation, star spots and faculae.

An example of the importance of modelling stellar activity is TRAPPIST-1. Interior structure models present a degeneracy between the composition of their volatile layer and the total mass of this layer. Transmission spectroscopy, which is affected by stellar activity, can break this degeneracy by revealing the chemical species in the atmosphere. In the case of TRAPPIST-1, Ducrot et al. (2018) used a photosphere and a low contribution of stellar spots at high temperature to model the stellar contamination in the transmission spectra. This

contamination model could not account for the inverted water line seen in the data, whereas the contamination model of Zhang et al. (2018) reproduced the water line. This contamination model considered that more than 50% of the stellar surface was covered by faculae and spots, which enable the formation of water vapour.

5 Conclusions

Our interior-atmosphere model can be applied to low-mass planets of a wide range of irradiations, including temperate planets with liquid and ice conditions to highly irradiated ones. We perform a spectroscopic analysis to obtain refined planetary masses and stellar parameters and abundances for the multiplanetary system K2-138 (Acuña et al. in prep) and apply our interior-atmosphere model to their planets. We find that the K2-138 system presents a WMF trend of increasing water content with incident flux for the inner planets, while the outer planets show a constant water content (a plateau). This trend is also seen in TRAPPIST-1 (Acuña et al. 2021) and could be the result of several formation mechanisms, including atmospheric mass loss, migration and location of accretion in the protoplanetary disk.

In addition, we conclude that stellar activity affects both planetary radius and transmission spectroscopy measurements, which are essential to break the degeneracy present in our interior structure models. We need accurate stellar activity models, including granulation, faculae and spots in transit photometry and transmission spectroscopy to help us identify planetary structure and composition trends.

M.D. and O.M. acknowledge support from CNES

References

Acuña, L., Deleuil, M., Mousis, O., et al. 2021, A&A, 647, A53
Agol, E., Dorn, C., Grimm, S. L., et al. 2021, The Planetary Science Journal, 2, 1
Brugger, B., Mousis, O., Deleuil, M., & Deschamps, F. 2017, ApJ, 850, 93
Brugger, B., Mousis, O., Deleuil, M., & Lunine, J. I. 2016, ApJ, 831, L16
Christiansen, J. L., Crossfield, I. J. M., Barentsen, G., et al. 2018, The Astronomical Journal, 155, 57
Czesla, S., Huber, K. F., Wolter, U., Schröter, S., & Schmitt, J. H. M. M. 2009, A&A, 505, 1277
Dorn, C., Khan, A., Heng, K., et al. 2015, A&A, 577, A83
Ducrot, E., Sestovic, M., Morris, B. M., et al. 2018, AJ, 156, 218
Gillon, M., Jehin, E., Lederer, S. M., et al. 2016, Nature, 533, 221
Lopez, T. A., Barros, S. C. C., Santerne, A., et al. 2019, A&A, 631, A90
Marcq, E. 2012, Journal of Geophysical Research (Planets), 117, E01001
Marcq, E., Salvador, A., Massol, H., & Davaille, A. 2017, Journal of Geophysical Research (Planets), 122, 1539
Mazevet, S., Licari, A., Chabrier, G., & Potekhin, A. Y. 2019, A&A, 621, A128
Mousis, O., Deleuil, M., Aguichine, A., et al. 2020, ApJ, 896, L22
Sotin, C., Grasset, O., & Mocquet, A. 2007, Icarus, 191, 337
Turbet, M., Bolmont, E., Ehrenreich, D., et al. 2020, A&A, 638, A41
Unterborn, C. T., Desch, S. J., Hinkel, N. R., & Lorenzo, A. 2018, Nature Astronomy, 2, 297
Wagner, F. W., Sohl, F., Hussmann, H., Grott, M., & Rauer, H. 2011, Icarus, 214, 366
Zhang, Z., Zhou, Y., Rackham, B. V., & Apai, D. 2018, AJ, 156, 178